cavities. As a consequence, the volumes of environmental pollutants released by the K-Pg impact will be better constrained, together with its role in causing the end-Cretaceous mass extinction (*37*). Because the deep subsurface biosphere is influenced by fracturing and mineralogical changes in host rocks induced by shock and post-impact hydrothermal activity, understanding how impact craters are formed and modify the environment will advance our understanding of deep subsurface life on Earth and potential habitability elsewhere.

The validation of the dynamic collapse model also strengthens confidence in simulations of large-crater formation on other planetary bodies. These simulations suggest that as crater size increases, the rocks that form peak rings originate from increasingly deeper depths (*38*). This relationship means that the composition of the peak-ring lithology provides information on the crustal composition and layering of planetary bodies and may be used to verify formation models, such as for the Moon (*6*, *38*, *39*). One of the principal observations used to support a version of the nested melt-cavity hypothesis in Baker *et al*. (*7*) is that peak rings within basins of all sizes on the Moon contain abundant crystalline anorthosite and must, therefore, originate from the upper crust, if indeed the lower crust is noritic. Our results suggest a deeper origin for peak-ring rocks and thus are more in accordance with alternative models for the composition of a heterogeneous lunar crust in which an anorthositic layer extends regionally to deeper depths (*40*, *41*). The dynamic collapse model and Expedition 364 results predict density reduction through shock and shear fracturing within the uplifted material (*33*), which is consistent with the recent Gravity Recovery and Interior Laboratory (GRAIL) mission results of a highly porous lunar crust (*42*) and the presence of mid-crustal rocks juxtaposed by shear zones in the peak ring at the Schrödinger crater (*38*). This linkage between deformation and overturning of material at the scales >10 km implies that over an extended period of time, impact cratering greatly increases the porosity of the subsurface and causes vertical fluxes of materials within the crust.

REFERENCES AND NOTES

1. H. J. Melosh, *Impact Cratering* (Oxford Univ. Press, 1989).
2. W. S. Hale, R. A. F. Grieve, *J. Geophys. Res.* **87** (S01), A65 (1982).
3. J. B. Murray, *Moon Planets* **22**, 269–291 (1980).
4. J. S. Alexopoulos, W. B. McKinnon, *Spec. Pap. Geol. Soc. Am.* **293**, 29 (1994).
5. M. J. Cintala, R. A. F. Grieve, *Meteorit. Planet. Sci.* **33**, 889–912 (1998).
6. J. W. Head, *Geophys. Res. Lett.* **37**, L02203 (2010).
7. D. M. H. Baker, J. W. Head, G. S. Collins, R. W. K. Potter, *Icarus* **273**, 146 (2016).
8. P. M. Vermeesch, J. V. Morgan, *Meteorit. Planet. Sci.* **39**, 1019–1034 (2004).
9. G. R. Osinski, J. G. Spray, *Meteorit. Planet. Sci.* **40**, 1813–1834 (2005).
10. A. Camargo-Zanoguera, G. Suarez-Reynoso, *Bol. Asoc. Mex. Geof. Expl.* **34**, 1 (1994).
11. J. V. Morgan *et al*., *Nature* **390**, 471 (1997).
12. A. R. Hildebrand *et al*., *Spec. Publ. Geol. Soc. Lond.* **140**, 155 (1998).
13. S. P. S. Gulick *et al*., *Nat. Geosci.* **1**, 131–135 (2008).
14. S. P. S. Gulick *et al*., *Rev. Geophys.* **51**, 31–52 (2013).
15. J. Brittan, J. Morgan, M. Warner, L. Marin, *Spec. Pap. Geol. Soc. Am.* **339**, 269 (1999).
16. J. V. Morgan, M. R. Warner, G. S. Collins, H. J. Melosh, G. L. Christeson, *Earth Planet. Sci. Lett.* **183**, 347–354 (2000).
17. B. Ivanov, *Sol. Syst. Res.* **39**, 381–409 (2005).
18. G. S. Collins *et al*., *Earth Planet. Sci. Lett.* **270**, 221–230 (2008).
19. G. L. Christeson *et al*., *Earth Planet. Sci. Lett.* **284**, 249–257 (2009).
20. L.E. Senft, S. T. Stewart, *Earth Planet. Sci. Lett.* **287**, 471–482 (2009).
21. Materials and methods are available as supplementary materials on *Science* Online.
22. T. Kenkmann, I. von Dalwigk, *Meteorit. Planet. Sci.* **35**, 1189–1201 (2000).
23. T. Kenkmann, G. S. Collins, K. Wünnemann, The modification stage of impact crater formation, *Impact Cratering* (Wiley-Blackwell, 2013).
24. A. Jahn, U. Riller, *Spec. Pap. Geol. Soc. Am.* **518**, 85–97 (2015).
25. R. A. F. Grieve, W. U. Reimold, J. Morgan, U. Riller, M. Pilkington, *Meteorit. Planet. Sci.* **43**, 855–882 (2008).
26. M. Pilkington, A. Hildebrand, C. Ortiz-Aleman, *J. Geophys. Res.* **99** (E6), 13147 (1994).
27. J. V. Morgan *et al*., *J. Geophys. Res.* **116** (B6), B06303 (2011).
28. G. Christeson, Y. Nakamura, R. T. Buffler, J. Morgan, M. Warner, *J. Geophys. Res.* **106** (B10), 21751–21769 (2001).
29. R. A. F. Grieve, F. Langenhorst, D. Stöffler, *Meteorit. Planet. Sci.* **31**, 6–35 (1996).
30. D. Lieger, U. Riller, R. L. Gibson, *Earth Planet. Sci. Lett.* **279**, 53–64 (2009).
31. U. Riller, D. Lieger, R. L. Gibson, R. A. F. Grieve, D. Stöffler, *Geology* **38**, 619–622 (2010).
32. G. S. Collins, *J. Geophys. Res.* **119**, 2600–2619 (2014).
33. F. Langenhorst, A. Deutsch, *Earth Planet. Sci. Lett.* **125**, 407–420 (1994).
34. A. C. Singleton, G. R. Osinski, P. J. A. McCausland, D. E. Moser, *Meteorit. Planet. Sci.* **46**, 1774–1786 (2011).
35. H. J. Melosh, *Impact and Explosion Cratering* (Pergamon Press, 1977).
36. W. B. McKinnon, *Lunar Planet. Sci. Conf. Proc.* **9**, 3965 (1978).
37. P. R. Renne *et al*., *Science* **339**, 684–687 (2013).
38. D. A. Kring, G. Y. Kramer, G. S. Collins, *Nat. Commun.* 10.1038/ncomms13161 (2016).
39. G. Y. Kramer, D. A. Kring, A. L. Nahm, C. M. Pieters, *Icarus* **223**, 131–148 (2013).
40. S. Yamamoto *et al*., *Geophys. Res. Lett.* **39**, L13201 (2012).
41. T. Arai, H. Takeda, A. Yamaguchi, M. Ohtake, *Earth Planets Space* **60**, 433–444 (2008).
42. M. A. Wieczorek *et al*., *Science* **339**, 671–675 (2013).

ACKNOWLEDGMENTS

This research used samples and data provided by IODP. Samples can be requested at http://web.iodp.tamu.edu/sdrm after the end of the moratorium on 19 October 2017. Expedition 364 was jointly funded by the European Consortium for Ocean Research Drilling (ECORD) and the International Continental Scientific Program, with contributions and logistical support from the Yucatan State Government and Universidad Nacional Autónoma de México (UNAM). G.S.C. was funded by UK Science and Technology Facilities Council grant ST/N000803/1. S.P.S.G. acknowledges his Fellowship at the Hanse-Wissenschaftkolleg, Germany. This is UTIG Contribution #3018.

SUPPLEMENTARY MATERIALS

www.sciencemag.org/content/354/6314/878/suppl/DC1
Material and Methods
Table S1
References (*43*–*63*)

27 July 2016; accepted 14 October 2016
10.1126/science.aah6561

ACTIVE MATTER

Command of active matter by topological defects and patterns

Chenhui Peng,* Taras Turiv,* Yubing Guo, Qi-Huo Wei, Oleg D. Lavrentovich†

Self-propelled bacteria are marvels of nature with a potential to power dynamic materials and microsystems of the future. The challenge lies in commanding their chaotic behavior. By dispersing swimming *Bacillus subtilis* in a liquid crystalline environment with spatially varying orientation of the anisotropy axis, we demonstrate control over the distribution of bacterial concentration, as well as the geometry and polarity of their trajectories. Bacteria recognize subtle differences in liquid crystal deformations, engaging in bipolar swimming in regions of pure splay and bend but switching to unipolar swimming in mixed splay-bend regions. They differentiate topological defects, heading toward defects of positive topological charge and avoiding negative charges. Sensitivity of bacteria to preimposed orientational patterns represents a previously unknown facet of the interplay between hydrodynamics and topology of active matter.

Swimming rodlike bacteria such as *Bacillus subtilis* show a distinct ability to sense and navigate their environment in search of nutrients. They propel in viscous fluids by rotating appendages called flagella, which are composed of bundles of thin helical filaments. Flagella can also steer the bacterium in a new direction by momentarily untangling the filaments and causing the bacterium to tumble (*1*). Alternating runs and tumbles of bacteria form a random trajectory reminiscent of a Brownian walk. The flows of the surrounding fluid created by bacteria cause their interactions and collective dynamics (*2*). Locally, the bacteria swim parallel to each other but globally this orientational order is unstable, showing seemingly chaotic patterns in both alignment of bacterial bodies and their velocities (*3*, *4*). Similar out-of-equilibrium patterns are met in many other systems, universally called "active matter" and defined as collections of interacting self-propelled particles, each converting internally stored or ambient energy into a systematic movement and generating coordinated collective motion (*5*–*7*). To extract useful work from the

Liquid Crystal Institute and Chemical Physics Interdisciplinary Program, Kent State University, Kent, OH 44242, USA.
*These authors contributed equally to this work. **†Corresponding author. Email: olavrent@kent.edu**

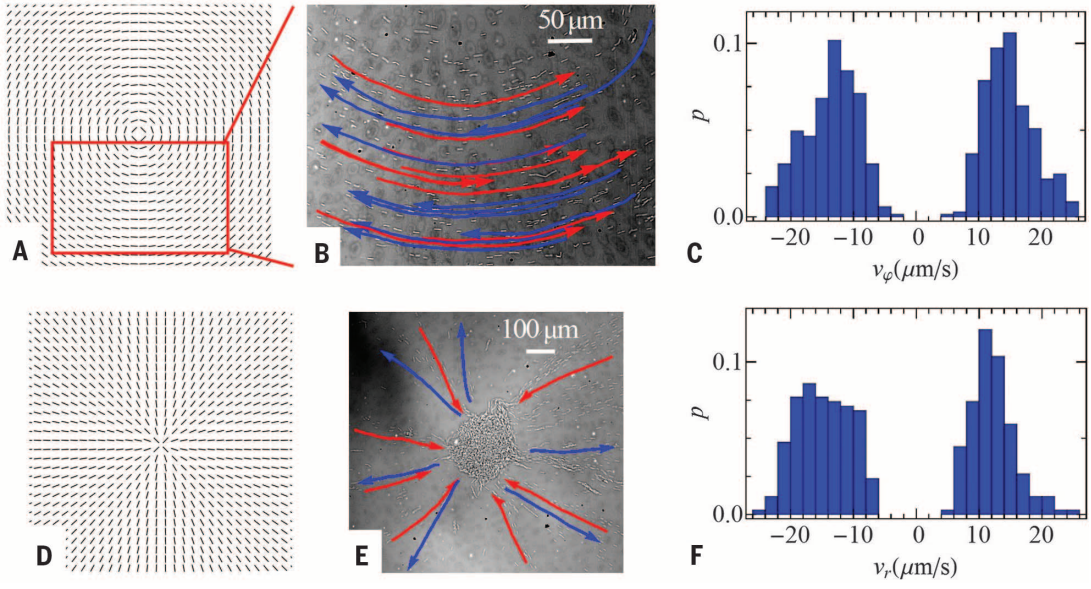

Fig. 1. Bipolar locomotion of bacteria in patterns of pure bend and pure splay. (**A**) Director pattern of a pure bend. (**B**) Circular trajectories of bacteria in the bend region. (**C**) Probability distribution (p) of azimuthal velocity (v_φ) of bacteria in the bend pattern. (**D**) Director field of pure splay. (**E**) Radial trajectories of bacteria moving toward and away from the center. (**F**) Probability distribution of radial velocities (v_r) of bacteria swimming in the splay pattern.

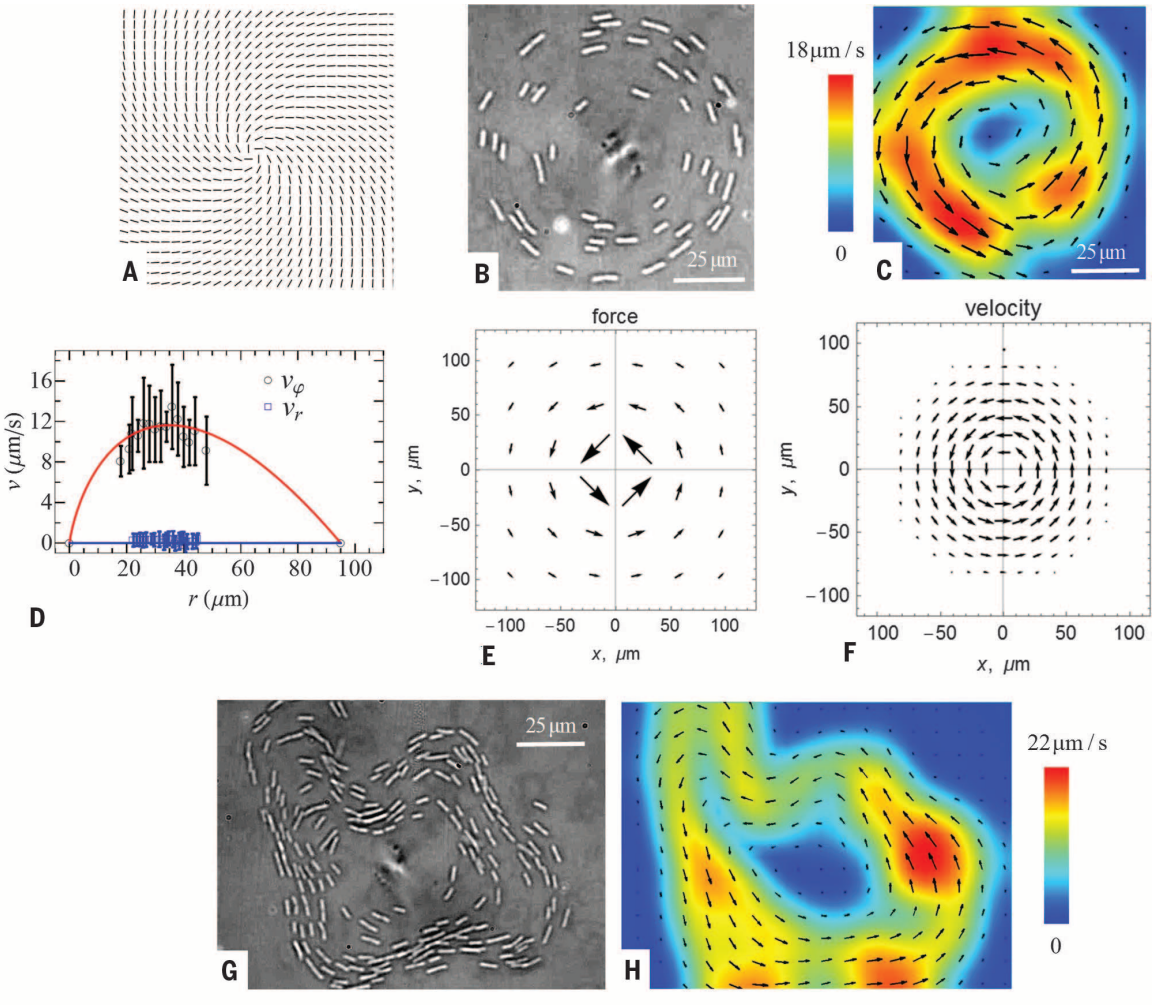

Fig. 2. Unipolar circular flow of bacteria around a spiraling vortex. (**A**) Mixed splay-bend director deformation of the vortex. (**B**) Circular bacterial swarm enclosing the vortex center. (**C**) Map of bacterial velocities. (**D**) Radial dependence of the azimuthal and radial velocities of the bacteria. Solid curves are predictions from Eq. 2. Error bars indicate SD taken for 40 bacteria. (**E**) Active force calculated from Eq. 1. (**F**) Velocity map calculated from Eq. 2. (**G**) Undulation instability of the circular swarm. (**H**) Velocity map in the undulating swarm.

chaotic dynamics of bacteria (or any other active matter) (*8*, *9*), one needs to learn how to control the spatial distribution of particles, as well as the geometry and polarity of their trajectories.

Placing swimming bacteria in an anisotropic environment of a nontoxic liquid crystal (*10*–*12*) might be one of the strategies to command active matter. Liquid crystals are anisotropic fluids, with a well-defined nonpolar axis of anisotropy called the director: $\hat{\mathbf{n}} \equiv -\hat{\mathbf{n}}$. A sphere moving in a liquid crystal parallel to the director enjoys the lowest viscous resistance (*13*, *14*). It has already been demonstrated

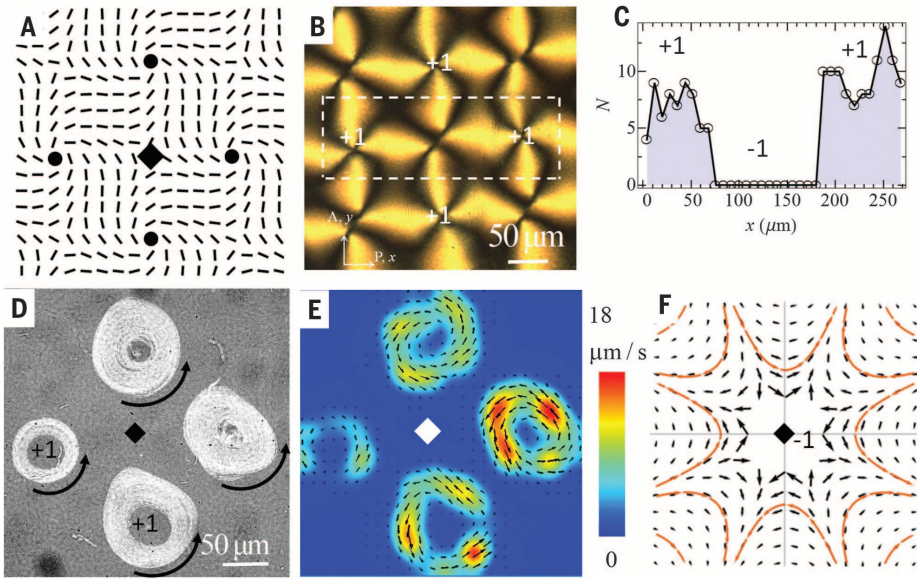

Fig. 3. Unipolar circular flows of bacteria in the periodic pattern of defects. (**A**) Director pattern with +1 (cores marked by circles) and –1 defects (one core marked by a diamond). (**B**) Polarizing optical microscopy texture of the pattern. A, analyzer; P, polarizer. (**C**) Spatial modulation of the number of bacteria (*N*) within the rectangular region in (B). (**D**) Counterclockwise trajectories of bacteria around four +1 spiraling vortices. (**E**) Map of corresponding velocities. (**F**) Active force calculated from Eq. 1 for a –1 defect.

that the liquid crystal director, either uniform (*10*–*12*) or spatially distorted (*11*, *15*), serves as an easy swimming pathway for bacteria. In particular, Zhou *et al.* (*11*) demonstrated curvilinear trajectories of bacteria around obstacles in a liquid crystal, while Mushenheim *et al.* (*15*) rectified the bacterial flows by using nematic cells with the so-called hybrid alignment at the opposite bounding plates. Liquid crystals were also used by Guillamat *et al.* (*16*) as an adjacent layer to an aqueous dispersion of active microtubules to align their active flows. Theoretical models of active systems with orientational order predict that a nonuniform director might cause polar flows (*17*, *18*). In particular, Green, Toner, and Vitelli (GTV) suggested that unidirectional flows in active nematics can be triggered by mixed splay-bend director deformations (*18*).

In this work, we produce spatially varying patterns of a liquid crystal anisotropic environment for swimming bacteria through controlled surface alignment of the director. The patterns are designed with well-defined deformations, either pure bend, pure splay, or mixed splay-bend. These preimposed patterns command the self-propelled bacteria dispersed in such a liquid crystal in a number of ways by controlling (i) geometry of trajectories, (ii) polarity of locomotion, and (iii) spatial distribution of bacterial concentration. Bacteria distinguish subtle differences in director deformations that occur over length scales much larger than their bodies. Namely, their swimming is bipolar in the pure-bend and pure-splay regions but unipolar in the mixed splay-bend case, matching the predictions of the GTV model (*18*). The bacteria also sense the topological charges of defects in the patterns, moving closer to defects of a positive topological charge and avoiding negative charges.

The patterned anisotropic environment represents thin (thickness d = 5 μm) slabs of a lyotropic chromonic liquid crystal (LCLC) confined between two flat glass plates. The LCLC is an aqueous dispersion of nontoxic disodium chromoglycate (*19*). The bounding plates are pretreated to impose the desired surface alignment of the adjacent LCLC (*20*–*22*). First, they are coated with a layer of photosensitive molecules. This layer is then irradiated with a light beam of linear polarization that changes from point to point, forcing the photosensitive molecules to align in accordance with local polarization. The photoaligned surface molecules align the director of the LCLC. The patterns are the same on the top and bottom plates so that the director is two-dimensional (2D).

In a homogeneously aligned liquid crystal, bacteria swim along $\hat{\mathbf{n}}$ in a bipolar fashion, half to the left and half to the right, so that there is no net flow (*11*, *12*, *15*). In the patterned cells with a pure bend (Fig. 1A) or a pure splay (Fig. 1D), the bacterial locomotion is very similar to the uniform case, being bipolar and parallel to the local $\hat{\mathbf{n}}$ (Fig. 1, B and E, and movies S1 to S3). When the number of bacteria in the radial splay configuration is low, they enter and leave the central region freely (movie S2), but if it is high, they accumulate into a concentrated immobilized

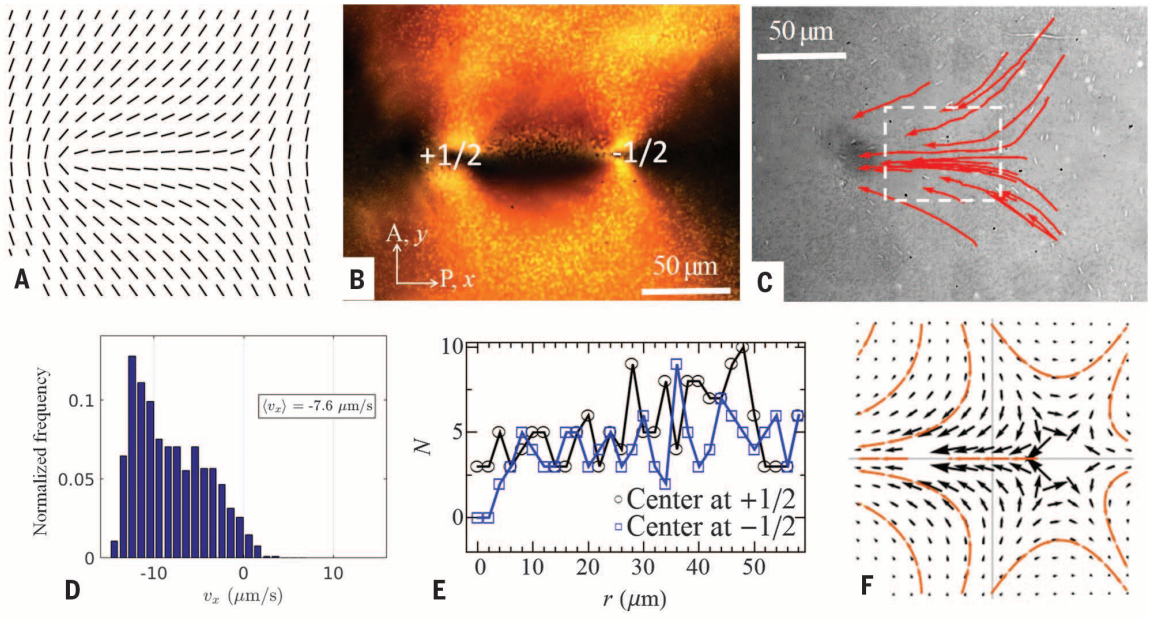

Fig. 4. Motion of bacteria controlled by a pair of semi-integer defects. (**A**) Predesigned director field. (**B**) Polarizing microscope texture of the defect pair. (**C**) Trajectories of bacteria moving predominantly from the –½ defect toward the +½ defect. (**D**) Polar character of velocities within the rectangular area shown in (C). (**E**) Concentration of bacteria versus radial distance from the center of the +½ and –½ defects. (**F**) Active force calculated for the pair, using Eq. 1.

disk-like colony (Fig. 1E and movie S3). In contrast, centers of circular bend remain bacteria-free (Fig. 1B and movie S1).

The bipolar swimming changes to unipolar when the bacteria encounter a pattern in the form of a spiraling vortex with mixed splay and bend (Fig. 2A and fig. S1). At any point, the local director $\hat{\mathbf{n}}$ makes an angle 45° with the radius-vector $\hat{\mathbf{r}}$, spiraling clockwise as one moves away from the center. The vortex is chiral, as it cannot be superimposed on its mirror image. The clockwise spiraling vortex forces counterclockwise circumnavigation of bacteria, producing a net flow (Fig. 2C and movie S4). The unipolar locomotion is along circular trajectories—that is, at 45° with respect to the surface-imposed $\hat{\mathbf{n}}$ (Fig. 2B)—which is in contrast to the cases of uniform, splayed, and bent director fields, where swimming is along $\hat{\mathbf{n}} \equiv -\hat{\mathbf{n}}$ (Fig. 1).

The spiraling vortex also controls bacterial concentration by attracting the bacteria to a circular annulus of a finite width. For example, a swarm of 50 bacteria occupies a region between radius $r \approx 15$ and 50 μm (Fig. 2B). The azimuthal velocity v_φ within the band is maximized at $r \approx 35$ μm (Fig. 2, C and D). As the number N of bacteria in the swarm increases (through the attraction of bacteria from outside regions) above a threshold of about $N_c = 110$, the circular trajectories start to undulate (Fig. 2, G and H). The undulations are similar to the periodic bend instability described for highly concentrated bacterial dispersions in a uniformly aligned LCLC (*11*).

Each spiraling vortex is a point defect of a topological charge $m = 1$ (*23*). The charge m is defined as the number of times the director rotates by 2π when one circumnavigates the defect (*23*); its sign reflects the direction of rotation with respect to the direction of circumnavigation. A periodic pattern of spiraling vortices with $m = 1$ and point defects with $m = -1$ is shown in Figure 3, A and B. The bacteria gather into circulating swarms around the $m = 1$ cores, all of which exhibit the same counterclockwise flow (Fig. 3, D and E, and movie S5).

Unipolar locomotion can also be designed as linear rather than circular. A defect pair with $m_1 = ½$ and $m_2 = -½$ is shown in Figure 4, A and B. The bacteria prefer to swim from the −½ defect toward the +½ defect rather than in the opposite direction (Fig. 4, C and D, and movie S6). The +½ defect is enriched with the bacteria, whereas the −½ defect is deprived of them (Fig. 4E).

The bacterial dynamics in a patterned LCLC shows a marked departure from the simple bipolar "swimming along $\hat{\mathbf{n}}$" behavior: (i) Bacteria can swim at some angle to the surface-imposed director (Figs. 2B and 3D). (ii) The locomotion becomes unipolar with the net flows of circular (Figs. 2, B and C, and 3, D and E) and linear (Fig. 4, C and D) type. Equally important is that (iii) the bacterial concentration varies in space substantially, being high around defects of positive topological charge and low at negative defects (Figs. 3C and 4E).

The emergence of unipolar locomotion in mixed splay-bend regions (Figs. 2 to 4) is in qualitative agreement with the GTV model (*18*), despite that fact that the model deals with an incompressible system whereas the experiment shows variation of bacterial concentration across the patterns. A combination of splay $\nabla\cdot\hat{\mathbf{n}}$ and bend $\hat{\mathbf{n}}\times\nabla\times\hat{\mathbf{n}}$ that satisfies the condition $\nabla\times[\hat{\mathbf{n}}\nabla\cdot\hat{\mathbf{n}}-\hat{\mathbf{n}}\times(\nabla\times\hat{\mathbf{n}})]\neq 0$ is predicted to produce a local guiding force (*18*)

$$\mathbf{f} = \alpha[\hat{\mathbf{n}}\nabla\cdot\hat{\mathbf{n}} - \hat{\mathbf{n}}\times(\nabla\times\hat{\mathbf{n}})] \qquad (1)$$

where $\alpha = c\sigma$ is the activity, defined by the concentration c of bacteria and the force dipole σ exerted by each swimmer on the fluid. For *B. subtilis*, σ is negative and estimated to be $\sigma \approx -1$ pN·μm in an aqueous environment (*24*). Although c varies across the patterns, we assume it is constant for a qualitative consideration. Eq. 1 applied to the clockwise spiral vortex in Fig. 2A, $\hat{\mathbf{n}} = \{\cos\theta, \sin\theta\}$, where $\theta = \tan^{-1}y/x - \pi/4$ (x and y are Cartesian coordinates), yields $\mathbf{f} = \{0, -\alpha/r\}$ [written in polar coordinates (r, φ): $r = \sqrt{x^2+y^2}$] (Fig. 2E). The flow velocity $\mathbf{v} = \{v_r, v_\varphi\}$ is obtained by balancing f with the viscous drag $\eta\nabla^2\mathbf{v}$

$$\mathbf{v} = \left\{0, \frac{\alpha r}{2\eta}\log\left(\frac{r}{r_0}\right)\right\} \qquad (2)$$

where r_0 is the distance at which the velocity vanishes, and η is the effective viscosity. When $\alpha < 0$, Eq. 2 predicts a counterclockwise circulation of bacteria around a clockwise vortex (Fig. 2F), which is in line with our observations (Figs. 2, B and C, and 3, D and E). The velocity field (Eq. 2) is similar to the velocity around an active gel vortex (*25*) and yields a nonmonotonous $v_\varphi(r)$, with a maximum $v_{max} = -\alpha r_0/2e\eta$ at $r = r_0/e$, matching qualitatively the experiment, in which $r_0/e = 35$ μm and $v_{max} \approx 12$ μm/s (Fig. 2D). The activity/viscosity ratio estimated from Eq. 2 is $\alpha/\eta \approx -0.7\ s^{-1}$.

The force (Eq. 1) calculated for the pair in Fig. 4F is directed from the −½ defect toward the ½ defect, reflecting the observed unipolar swimming from −½ to +½ in Fig. 4C. The force around the −1 defect deflects away from its center (Fig. 3F), again in a qualitative agreement with the observed bacterial avoidance of negative topological charges. For pure splay and pure bend 2D samples, the GTV model (*18*) predicts $\mathbf{f} = 0$ and, thus, no net flows, as in Fig. 1, which shows only bipolar swimming. A more detailed analysis should account for spatial variations of concentration and activity, potential flow-induced realignment of the director, anisotropy, and variations of effective viscosities.

The unipolar locomotion of bacteria is observed at relatively low concentration and, thus, low activity. For example, in the circulating swarm in Figs. 2B and 3D, $c \approx 1.4 \times 10^{15}\ m^{-3}$. This concentration is well below the critical threshold of instabilities described by Zhou *et al.* (*11*) for highly concentrated bacterial dispersions that exhibit undulations and topological turbulence. As the circular swarms attract more bacteria, increasing c by a factor of 2 or 3, the trajectories start to develop bend undulations (Fig. 2G), signaling that the activity overcomes the stabilizing liquid crystal elasticity (*11*).

To summarize, we demonstrate an approach to control active matter through a patterned anisotropic environment. Self-propelled bacteria sense the imposed patterns of orientational order by adapting their spatial distribution, heading toward topological defects of positive charge and avoiding negative charges, and switching from bipolar locomotion in splayed and bent environments to unipolar locomotion in mixed splay-bend regions. The demonstrated command of active matter by a spatially varying anisotropic environment opens opportunities for designing out-of-equilibrium spatiotemporal behavior, with the goal of developing new dynamic materials and systems.

REFERENCES AND NOTES

1. E. Lauga, *Annu. Rev. Fluid Mech.* **48**, 105–130 (2016).
2. D. L. Koch, G. Subramanian, *Annu. Rev. Fluid Mech.* **43**, 637–659 (2011).
3. C. Dombrowski, L. Cisneros, S. Chatkaew, R. E. Goldstein, J. O. Kessler, *Phys. Rev. Lett.* **93**, 098103 (2004).
4. A. Sokolov, I. S. Aranson, J. O. Kessler, R. E. Goldstein, *Phys. Rev. Lett.* **98**, 158102 (2007).
5. T. Vicsek, A. Czirók, E. Ben-Jacob, I. Cohen, O. Shochet, *Phys. Rev. Lett.* **75**, 1226–1229 (1995).
6. J. Toner, Y. H. Tu, S. Ramaswamy, *Ann. Phys.* **318**, 170–244 (2005).
7. D. Nishiguchi, K. H. Nagai, H. Chaté, M. Sano, https://arxiv.org/abs/1604.04247 (2016).
8. A. Sokolov, M. M. Apodaca, B. A. Grzybowski, I. S. Aranson, *Proc. Natl. Acad. Sci. U.S.A.* **107**, 969–974 (2010).
9. R. Di Leonardo *et al.*, *Proc. Natl. Acad. Sci. U.S.A.* **107**, 9541–9545 (2010).
10. A. Kumar, T. Galstian, S. K. Pattanayek, S. Rainville, *Mol. Cryst. Liq. Cryst.* **574**, 33–39 (2013).
11. S. Zhou, A. Sokolov, O. D. Lavrentovich, I. S. Aranson, *Proc. Natl. Acad. Sci. U.S.A.* **111**, 1265–1270 (2014).
12. P. C. Mushenheim, R. R. Trivedi, H. H. Tuson, D. B. Weibel, N. L. Abbott, *Soft Matter* **10**, 88–95 (2014).
13. J. C. Loudet, P. Hanusse, P. Poulin, *Science* **306**, 1525 (2004).
14. T. Turiv *et al.*, *Science* **342**, 1351–1354 (2013).
15. P. C. Mushenheim *et al.*, *Soft Matter* **11**, 6821–6831 (2015).
16. P. Guillamat, J. Ignés-Mullol, F. Sagués, *Proc. Natl. Acad. Sci. U.S.A.* **113**, 5498–5502 (2016).
17. R. Voituriez, J. F. Joanny, J. Prost, *Europhys. Lett.* **70**, 404–410 (2005).
18. R. Green, J. Toner, V. Vitelli, https://arxiv.org/abs/1602.00561 (2016).
19. C. J. Woolverton, E. Gustely, L. Li, O. D. Lavrentovich, *Liq. Cryst.* **32**, 417–423 (2005).
20. See supplementary materials on *Science* Online.
21. Y. Guo *et al.*, *Adv. Mater.* **28**, 2353–2358 (2016).
22. C. Peng *et al.*, *Phys. Rev. E* **92**, 052502 (2015).
23. M. Kleman, O. D. Lavrentovich, *Soft Matter Physics: An Introduction* (Springer, 2003).
24. K. Drescher, J. Dunkel, L. H. Cisneros, S. Ganguly, R. E. Goldstein, *Proc. Natl. Acad. Sci. U.S.A.* **108**, 10940–10945 (2011).
25. K. Kruse, J. F. Joanny, F. Jülicher, J. Prost, K. Sekimoto, *Phys. Rev. Lett.* **92**, 078101 (2004).

ACKNOWLEDGMENTS

We thank S. Zhou and G. Cukrov for help with experiments and I. Aronson and A. Sokolov for discussions. This work was supported by NSF grants DMR-1507637 (design and development of patterned alignment), DMS-1434185 (analysis of dynamics), and CMMI-1436565 (design and fabrication of metamasks). C.P. and T.T. performed the experiments. O.D.L. conceived and directed the research. Y.G. and Q.-H.W. provided the metamasks. C.P., T.T., and O.D.L. analyzed the data. All authors participated in discussing and writing the manuscript.

SUPPLEMENTARY MATERIALS

www.sciencemag.org/content/354/6314/882/suppl/DC1
Materials and Methods
Supplementary Text
Figs. S1 and S2
References (*26*–*29*)
Movies S1 to S6

1 August 2016; accepted 21 October 2016
10.1126/science.aah6936

Command of active matter by topological defects and patterns

Chenhui Peng, Taras Turiv, Yubing Guo, Qi-Huo Wei, and Oleg D. Lavrentovich

Science, **354** (6314), .
DOI: 10.1126/science.aah6936

Directing traffic with patterns

Biological entities, such as bacteria, may direct their motion in response to their environment, but this usually does not lead to large-scale patterns or collective behavior. Peng *et al.* found that the orientational ordering of a liquid crystal could direct the flow of self-propelling bacteria, which in turn influenced the patterning of the liquid crystal molecules. Patterns on a substrate caused surface anchoring of the liquid crystals that transmitted to the ordering of the bacteria, thus imparting control on what would otherwise be chaotic out-of-equilibrium behavior.

Science, this issue p. 882